Electrochemical CO_2 reduction for Syngas production on ZnO/CNT catalysts

Ida Hjorth[1], Yalan Wang[1], Yahao Li[1], Marthe Emelie Melandsø Buan[2], Magnus Nord[3], Magnus Rønning[1], Jia Yang[1] and De Chen[1]

[1]Department of Chemical Engineering, Norwegian University of Technology and Science

[2]Department of Chemistry and Materials Science, Aalto University

[3]School of Physics and Astronomy, University of Glasgow

Abstract: Electrochemical reduction of CO_2 and H_2O can provide a promising pathway to synthesis gas generation for renewable electric energy storage and fuel production with the closed anthropogenic carbon cycle. However, the lack of affordable highly active catalysts to activate the stable CO_2 and H_2O molecules presents a substantial challenge. Here we report ZnO supported on nanocarbon as a cost-effective and active catalyst for selective conversion of CO_2 and H_2O to predominately synthesis gas, with higher selectivity and activity compared to polycrystalline metal catalysts such as Ag and Cu. The H_2/CO ratio can be tailored for different industrial processes by tuning the applied potential and the particle size of ZnO. Density functional theory calculations showed that the higher activity of ZnO is related to more significantly stabilized intermediates, CO_2*, COOH, and CO* compared to Cu and Ag. Our results highlight a promising class of low-cost, abundant oxide as active electrocatalysts for synthetic fuel production from CO_2.

1. Introduction

Natural photosynthesis typically converts H_2O and CO_2 to sugars for energy storage. Artificial photosynthesis can accelerate this process, be more energy efficient than the use of biomass [1], and has no food vs fuel controversy concerning land use. Electrochemical conversion of CO_2-saturated water powered by renewable electricity is one way of achieving artificial photosynthesis, and a possible strategy for renewable and sustainable production of fuels and chemicals [2,3]. It has the benefit of direct utilization of renewable electricity and an abundant, inexpensive and non-toxic proton source (water). If H_2 evolves from water-splitting while CO_2 is reduced to CO, synthesis gas can be produced in a one-step process. Given a controllable H_2/CO composition, the product stream can be suitable for exothermic downstream

processing [4], to products such as methanol, Fischer-Tropsch fuels etc. The exothermic nature of these downstream reactions suggests an energy-efficient pathway for chemicals and fuels without additional energy input. Although CO_2 can be electrochemically converted to liquid alcohols and hydrocarbons, the low concentration of the products in electrolyte makes product separation extremely challenging, and a process via synthesis gas can be more energy and cost-efficient.

Because of relatively low efficiency, low reaction rates and high cost limiting electrochemical CO_2 reduction (ECR) [2,5], catalyst development is playing a more and more important role to improve the process [6]. Important electrochemical catalyst properties are high catalytic surface area, good electronic conductivity, activity, stability, product selectivity and cost. Gold [7,8] and silver [9,10] are transition metal catalysts receiving much attention due to their high selectivity for CO in ECR. A few reports have shown that also Zn has an ability for ECR, giving mainly CO or formic acid [11-13]. Therefore, Zn may provide a low-cost alternative to gold and silver catalysts. Another aspect in the design of the catalyst is the oxidation state of the material, as oxidized or partially oxidized metals have shown interesting activity for ECR. Gold and copper catalysts derived from the corresponding oxide showed better selectivity or activity than their maternal metal foil equivalents [7,14].

In this work, we report for a highly dispersed ZnO on carbon nanotubes (CNTs) as efficient catalysts for ECR to synthesis gas, with tuneable H_2 /CO composition favorable for production of hydrocarbons by Fischer-Tropsch synthesis. Our study provides a material class as a potentially cost-efficient alternative to Au and Ag catalysts for ECR at relatively low overpotentials. Density Functional Theory (DFT) calculations were performed to rationalize the higher activity of CO_2 reduction on ZnO compared to Ag (111) and Cu (111). CNTs were used as electrocatalyst supports analogous to fuel cell electrocatalysts [15], due to the large surface area and excellent electronic conductivity of this material. ZnO was uniformly deposited on the CNTs by impregnation with a metal-complex solution. The ZnO formed by the decomposition of the precursor has good wettability to the CNT surface, thus enhancing the dispersion of ZnO [16,17]. Another advantage of this support material is the mesoporous

structure which enhances mass transport compared to microporous materials [18-20]. The effect of ZnO particle size on the synthesis gas formation is also addressed.

2. Materials and Methods

2.1. Catalyst preparation

Commercial carbon nanotubes (CNT) from Chengdu were purified and oxidized by heating in concentrated HNO_3 at reflux conditions for 2 hours. This treatment was repeated 3 times, the CNTs were washed with distilled water in between - and with copious amount of distilled water after the last repetition. The purified fibers were dried at 110 ◦C overnight, and mortared into a powder. ZnO was coated on the oxidized CNTs by impregnation with a metal-complex solution [1, 2], and the target loading was 20 wt% ZnO. The amount of liquid needed to fill the pores of the CNT powder was measured by simply adding it to the support until liquid appeared on the surface. A Zn(NO3)2 · 6 H2O precursor was dissolved together with citric acid (CA) and ethylene glycol (EG) in equal molar amounts, in the required amount of water. This metal-complex solution was immediately used to impregnate dry CNT powder. The material was dried at 110°C overnight and calcined in air. After the calcination, the solids were mortared. Parts of the sample was then annealed in argon flow at different temperatures to stimulate particle sintering and growth. Catalysts with different ZnO particle sizes were prepared by thermal treatment the ZnOCNT in argon atmosphere at various temperatures.

2.2 Catalyst characterization

The catalyst powders were examined with a Bruker D8 Advance DaVinci X-ray Diffractometer with MoKα radiation, in a variable slit mode. In EVA, the background was subtracted and a fixed slit mode was simulated such that Rietveldt refinement in TOPAS could be used for calculating the Scherrer crystallite sizes.

The catalysts were imaged with a Hitachi S-5500 S(T)EM microscope, and both Dark Field and Bright Field images were taken. With ImageJ, particle sizes were measured in several images, as well as wetting angles of particles situated on the tube edges.

The used catalyst was examined with EELS in an aberration corrected Scanning Transmission Electron Microscope. Both low-loss and high-loss spectra were recorded, and the energy scale was calibrated by aligning the zero-loss peak. HyperSpy [9] was used to analyze the spectra. After background removal, noise in the high-loss spectrum was reduced with Principal Component Analysis. The models of zinc and oxygen were created by fitting a Hartree-Slater cross sections to the respective adsorption edge.

Immediately after ECR, a used catalyst was recovered from the electrode by ultrasonication of the electrode tip in ethanol. In this ECR test a rotating disk electrode setup was used. The used catalyst was transferred to a sample holder and examined with Raman Spectroscopy. A HORIBA Jobin Yvon, model HR800 UV was used with a 633 nm source.

2.3 Electrochemical testing

A Nafion membrane separated the anolyte and catholyte in the electrochemical cell. The anolyte, 230 mL 0.1 M $KHCO_3$ was vigorously purged with CO_2 for 10 minutes and injected into the electrochemical cell under CO_2 bubbling. The catholyte, 70 mL 0.1 M $KHCO_3$ (ultrapure from Sigma Aldrich) was vigorously purged with CO_2 for 5 minutes, and injected into the electrochemical cell under 10.1 mL/min CO_2 bubbling. A Ag/AgCl electrode was used as reference, and a platinum mesh as counter electrode. The catholyte compartment was connected to a micro-GC for analyzing the product gases online.

The measurement program was started right after the catholyte injection. A sequence of chronopotentiometric measurements were performed, with increasing reduction currents. The current was kept constant at each level for 30 minutes. In between these segments, a short impedance measurement was performed to determine the solution resistance for iR-compensation. The GC sampled the product gas flow with approximately 3 minutes intervals, and the average of these samples at each level is used. In some figures, error bars are indicated and these are based on the standard deviation of the GC-samples at the respective level. Long term ECR stability test was performed on a ZnOCNT catalyst for 4 hours at 2.9 mA/cm^2.

The faradaic efficiency (FE) is defined as

$$FE = \frac{I_p}{I_{tot}} \qquad (2)$$

And the energy efficiency is defined as in [5]

$$EE = \frac{FE \cdot E^0}{E^0 + \eta} \quad (3)$$

$$E^0_{H2} = 1.23$$

$$E^0_{CO} = 1.33$$

Where I_p is partial current and I_{tot} is total current, E^0 is equilibrium potential, η is over potential.

3. Results and discussion

Catalysts with different ZnO particle sizes were successfully prepared by thermal treatment the ZnOCNT in argon atmosphere at various temperatures. Besides providing thermal energy for particle agglomeration to occur, the heating in inert atmosphere caused carbon thermal reduction of ZnO. Using X-ray diffractograms (Figure S1) carbon and hexagonal ZnO (wurtzite) were identified as the dominant phases in the ZnOCNT catalysts. A minor metallic zinc phase emerged in the X-ray diffractogram of the ZnOCNT sample annealed at 580 °C (Figure S1). In the sample annealed at 750 °C no zinc phases were detected. Temperature programmed reduction of ZnOCNT in argon (Figure S2) showed that the thermal reduction of ZnO occurred at temperatures above 550 °C, where oxygen from ZnO is rejected as CO. The maximal degree of ZnO reduction to Zn was quantified by using the thermogravimetric data (Table 1). Up to 580 °C it was assumed that no Zn evaporation occurred, as the loading of ZnO found by TPO was unchanged. Around 700 °C, the sample started to lose a substantial amount of weight. Metallic zinc is liquid with a high vapor pressure at this temperature. Zn evaporation was confirmed by TPO of ZnOCNT catalyst heat-treated at 750 °C, which showed that no ZnO was left on the CNTs. Traces of nickel were present in all samples, and elemental mapping in Scanning Transmission Electron Microscopy (STEM) established that it is a residual from CNT growth, that did not completely dissolve in the CNT purification step.

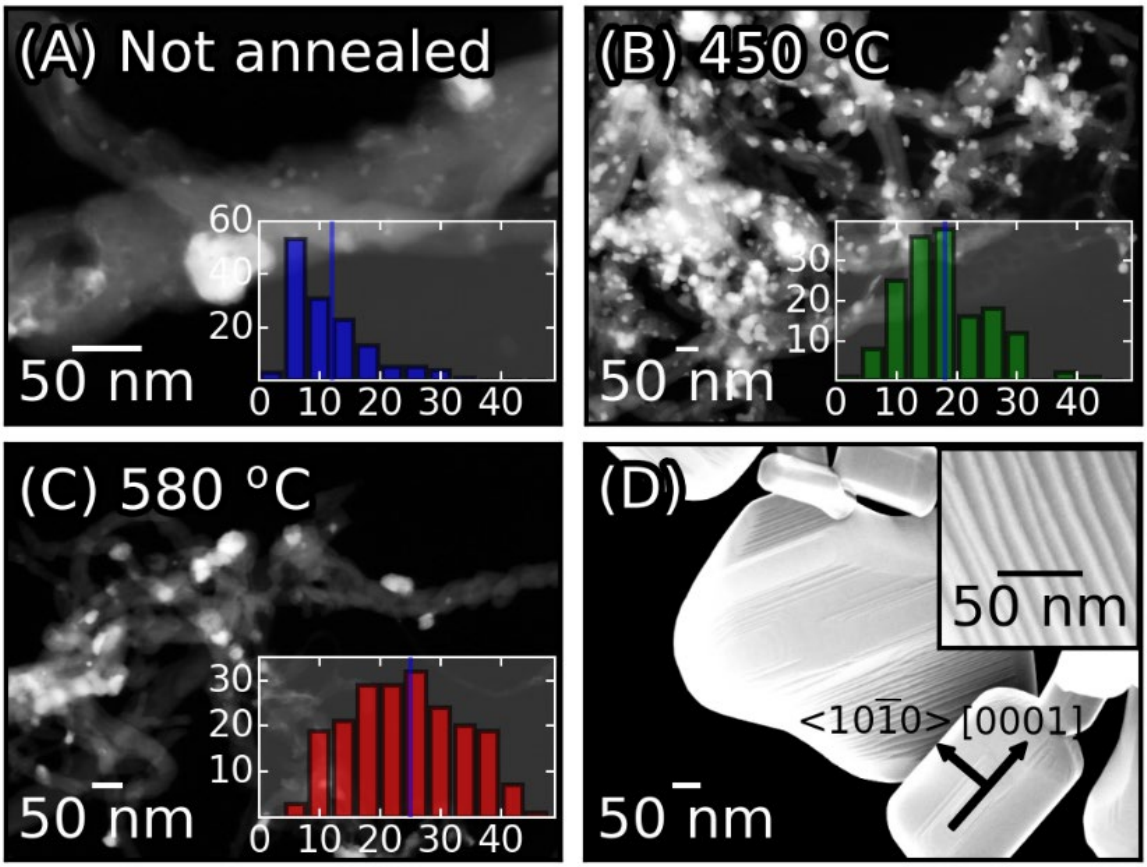

Figure 1. (a-c) STEM images of the ZnOCNT catalysts, with particle size distribution insets. (d) SEM image of commercial ZnO powder, with crystallographic directions, annotated on one particle based on the typical shape [21,22].

Table 1. Material properties for CNT, ZnO powder and ZnOCNT catalysts, not annealed and annealed in argon at 450°C and 580°C

		ZnOCNT		ZnO	CNTox
Annealing	-	450°C	580°C	-	-
Scherrer cryst. size[a]	15.6	19.4	23.8	-	-
STEM mean particle size[a]	12	18	25	100 - 500	-
ZnO loading [wt%][b]	19.0	19.6	18.5	100	0
Metallic zinc%	0	0	8	0	-
BET surface area[c]	111	99	85	4	114
Modelled relative geometric ZnO surface	4.5	3.8	2.6	1.0	-

[a] in nm, [b] Temperature Programmed Oxidation (TPO), [c] m^2/g

Further imaging of fresh catalysts with STEM showed that ZnO particles mostly decorated the outside of the CNTs, but some particles were located on the inside. The mean ZnO particle diameter found by STEM imaging was similar to the crystallite size obtained from XRD, see

Table 1. However, on the non-annealed catalyst, the average particle size was smaller than the mean, in the range of 4-8 nm. When the annealing temperature was increased, the particle size increased and the size distribution changed, as seen in Figure 1. The commercial ZnO powder had a broad distribution of larger particle sizes (100-500 nm).

ZnOCNT, ZnO powder and CNTs were tested for synthesis gas production through ECR in 0.1 M $KHCO_3$. Partial CO and H_2 currents for the ZnOCNT catalysts are shown in Figure 2. The syngas formation performance of the non-annealed ZnOCNT catalyst in this work is just as good as on a polycrystalline Ag foil [10], when producing synthesis gas with 1:1 CO:H_2 at a similar applied potential.

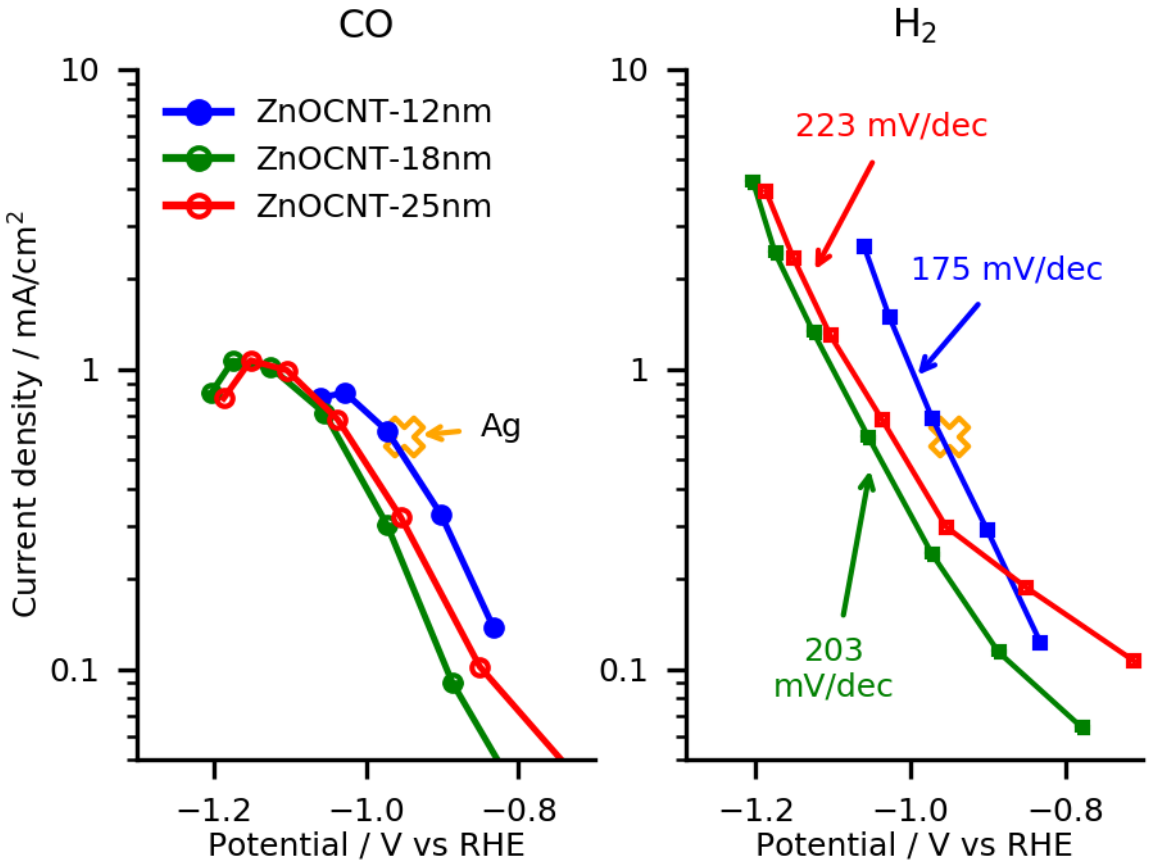

Figure 2. CO and H_2 partial currents on ZnOCNT annealed in argon at 580 °C (25 nm), 450 °C (18 nm) and not annealed (12 nm). Synthesis gas formation with a 1:1 composition is compared with polycrystalline Ag, from work by Ma et al [10].

In Figure 2 it is seen that the onset of ECR to CO on the annealed catalysts was about 100 mV more negative than the onset on the non-annealed ZnOCNT catalyst. The smaller ZnO crystals (12nm) obviously resulted in a higher current compared to larger one (18nm). Similar size

dependence was also found for hydrogen evolution. The Tafel slope for the H_2 evolution reaction (HER) is decreasing with ZnO particle size. A low Tafel slope means that the reaction rate is more sensitive to changes in the potential, which is in generally good for the kinetics of the reaction. The better activity of smaller ZnO crystals can be ascribed to the improved electronic conductivity of the catalyst, and it has been reported that the potential shift at 1 mA/cm^2 can be in the range of 21 mV per nm of oxide [23]. Another possible reason for the improved activity on smaller ZnO particles might be more low-coordinated sites for CO_2 and H2O activation. However, a slightly higher activity was found on 25 nm than 18 nm ZnO, possibly due to coexisting of Zn and ZnO on 25 nm catalysts obtained by high temperature annealing.

Besides the difference in onset and H_2 Tafel slopes, a similar potential dependent behavior was observed for all samples. As the overpotential was increased the evolution of both products increased, until the evolution of CO peaked and started to decline at approximately 1 mA_{CO}/cm^2. One difference was observed, which was the enhanced activity for HER on ZnOCNT-580 °C in the lower overpotential region. This enhancement was possibly due to better site activity on metallic zinc in this potential region. From temperature programmed reduction, it was found that up to 8 % of the zinc in this catalyst was metallic (Table 1). The "kink" at -1 V is indicative of a change in reaction mechanism.

The faradaic and energy efficiency for the ZnOCNT catalysts is shown in Figure 3. Selectivity to synthesis gas in the gas phase was in general high, while the energy efficiency was moderate. A small decline in faradaic and energy efficiency was observed from the non-annealed catalyst with 12 nm average particle size, to the catalyst annealed at 450 °C (18 nm). When annealed at 580 °C (25 nm) the efficiency at the lower overpotential was higher, due to the improved selectivity and activity for water splitting to H_2 in this region. The syngas composition as a function of electrode potential was shown in the supporting information Figure S10.

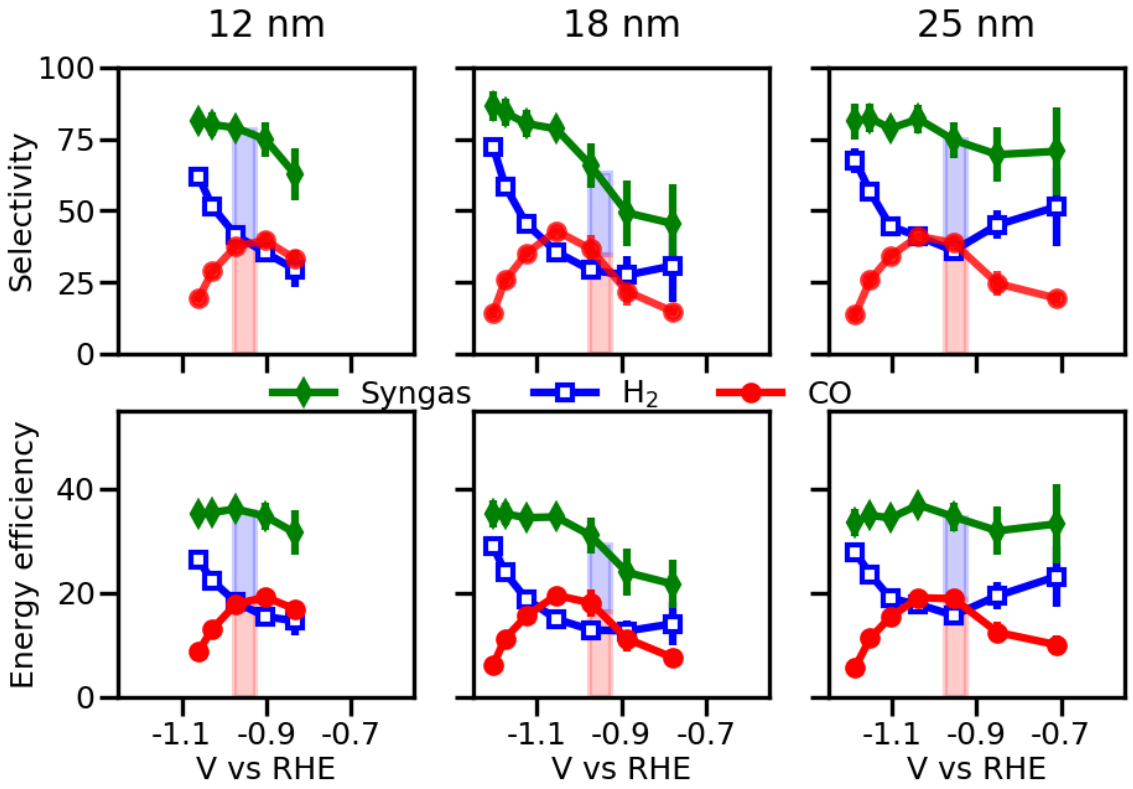

Figure 3. Faradaic and energy efficiency for synthesis gas on ZnOCNT catalysts. The efficiency for CO (red) and H_2 (blue) at -0.95 V is emphasized with bars for easier visual comparison.

It is little confusing using faradaic efficiency and selectivity. It is better using faradaic efficiency in the plot

To further evaluate active electrochemical CO_2 reduction on both porlar and non-polar ZnO surfaces and compare it to conventional Cu and Ag catalysts, DFT calculations were carried out on ZnO, Cu and Ag. The results at 0 V vs RHE are shown in Figure 4. The CO_2 electroreduction intermediates COOH* and CO_2* are more stabilized on both O terminated polar ZnO (0001) and non-polar ZnO (1010), compared to Ag(111) and Cu(111). Tridentate carbonates and bidentate carbonate formed after CO_2 adsorption on non-polar ZnO(1010) and polar ZnO(0001), respectively, shown in Fig. S12 in the supplementary information. The polar ZnO surface has a lowest free energy for the CO_2 conversion, which strongly implies that ZnO (0001) is more active than Ag and Cu for CO_2 conversion. The non-polar ZnO surface binds OH less strongly than the polar surface, leading to a different characteristic of the free energy curve

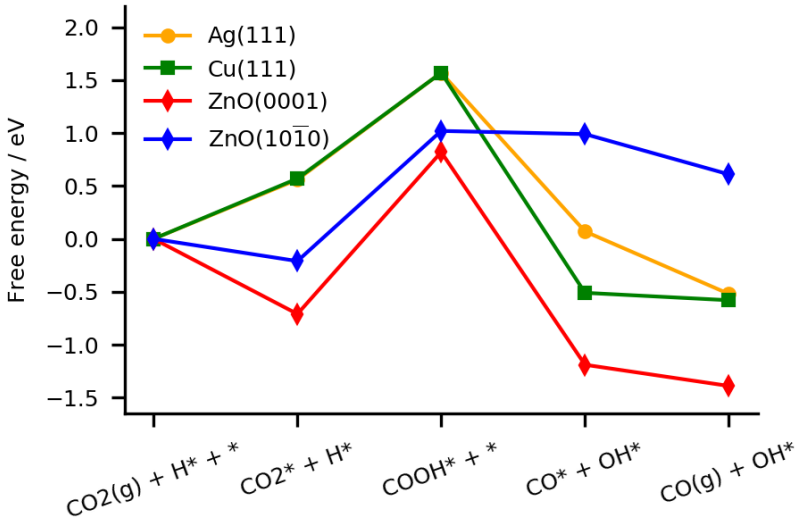

Figure 4: Free energy for CO_2 conversion to CO on ZnO, gold and silver.

At negative electrode bias, oxygen vacancies may be created through OH-removal, and the electron density on the surface will be high. This may facilitate active sites for CO_2 dissociation on polar ZnO surfaces[24]. It was found that smaller ZnO particle sizes better wetted the CNT surface (Figure S2), and that most of the particles had symmetric wetting angles, meaning perpendicular (0001)-planes on the CNT-surface[17]. This could result in smaller particles having relatively more of the polar surface exposed, and it is expect to facilitate the CO_2 activation.

To further study the effect of particle size on ECR, and the possible enhancement of ECR on polar planes, partial currents were normalized with respect to surface area, which was geometrically modeled by a method described in the supporting information. Commercial ZnO powder with coarse particles was also tested for ECR. The current normalized with respect to ZnO surface area is shown in Figure 5 (a). Consistent with the above hypothesis, it was observed that the ZnO powder had the highest CO formation rate per ZnO surface area, and maximal CO formation increased with increasing particle size looks like opposite to what discussed above?? . The improved CO evolution can also be a direct effect of the difference in HER, which may compete with CO_2 reduction. HER has the opposite particle size relationship - the tafel slope increases with increasing particle size. Also, an improved mass

transfer due to the much thinner bulk ZnO catalyst layer compared to the supported catalysts can give enhanced CO formation on the powder sample. The difference in catalyst layer thickness may be 1-2 orders of magnitude.

The ZnOCNT catalysts will have a varying degree of exposed carbon. To identify any possible influence of more exposed carbon, oxidized CNTs without ZnO, as well as pure ZnO was tested. Figure 5 (b) shows the results, together with two of the ZnOCNT catalysts. The current was normalized with respect to the relative mass of either CNTs or ZnO.

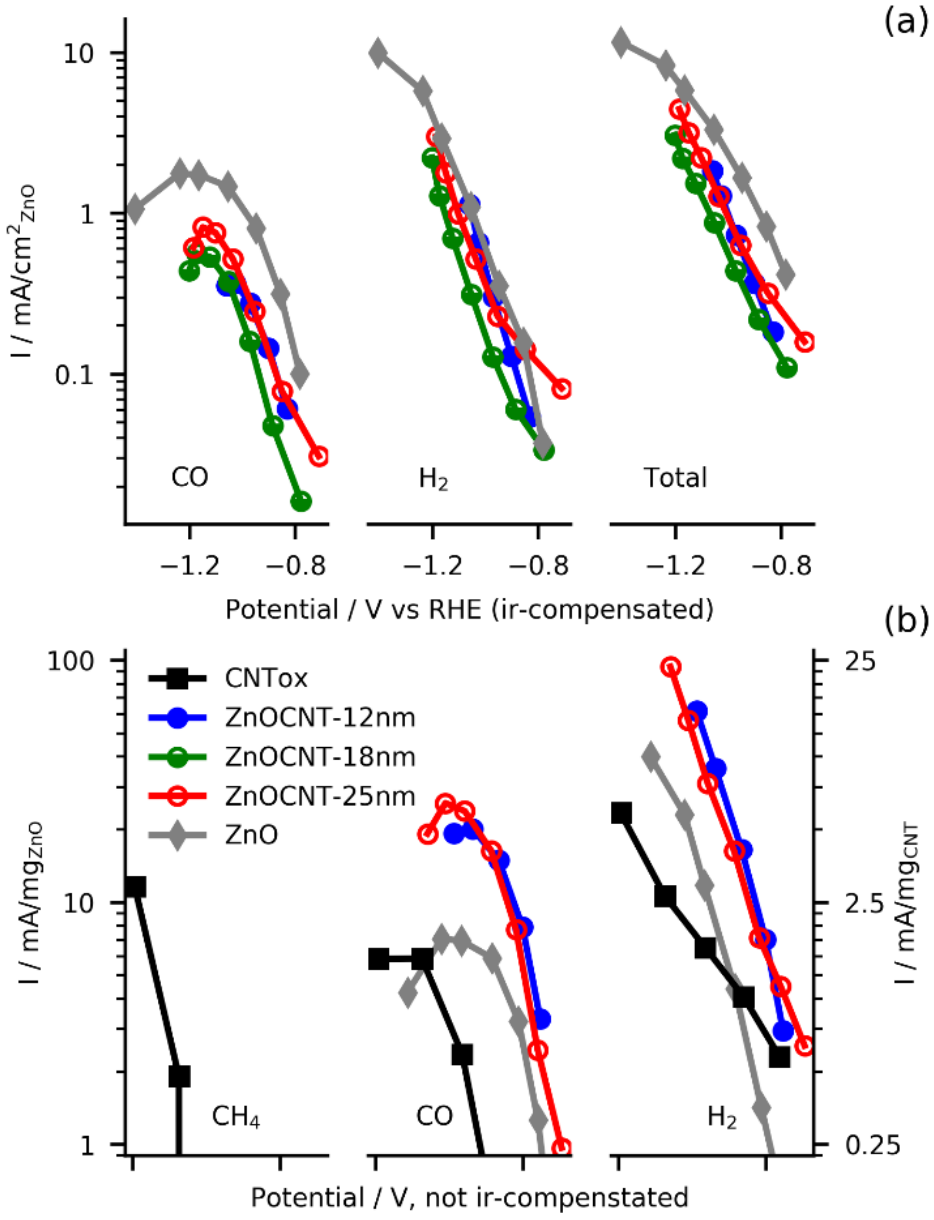

Figure 5. (a) The partial and total currents normalized with respect to modeled ZnO surface area. (b) H_2, CO and CH_4 for CNT, ZnO powder and ZnOCNT, normalized with respect ZnO and CNT mass.

It is clear that the activity of ZnO was much higher than the CNT support, but only the CNTox showed significant methane evolution. The activity of the CNTs for ECR may be due to presence of metal impurities[25]. Per mass of ZnO, the activities of the supported catalysts were significantly higher than the ZnO powder. The ZnO catalyst layer is much thinner than the ZnOCNT layer and the difference is therefore not due to internal mass transfer limitations in the ZnO powder, but rather the much lower dispersion and poorer electronic conductivity.

In Figure 6 long term ECR on ZnOCNT is demonstrated, showing that the H_2:CO ratio over time increased to 2:1 or higher. This is a composition well suited for downstream processing. Depletion of H^+ in the catholyte may influence the observed selectivity, but changes in the catalyst material can also occur - such as reduction of oxide to metal at highly negative potentials[12]. To investigate the material stability during ECR, a used ZnOCNT catalyst was collected and characterized with Raman and X-ray photoelectron spectroscopy without being stored in air. Compared to the original catalyst the Raman spectra (Figure S7) were unchanged, and the position of the Auger LMM peak relative to the Zn $2p_{2/3}$ peak (giving the modified Auger parameter α') excluded formation of metallic zinc[26]. This showed that Zn was still in an oxidized form after the reaction. Electron Energy Loss spectra (EELS) of the oxygen K-edge were consistent with the fine structure of oxygen in ZnO[27]. Furthermore, by analysing the used electrolyte with ICP-MS it was established that no leaching of Zn had occurred. All this is in agreement with Pourbaix diagrams predicting that ZnO is the stable passive phase of Zn in water[28].

However, STEM images of the used catalyst showed particles with better wetting of the carbon surface, and smaller size. Before ECR on the non-annealed ZnOCNT the average particle size was 4-8 nm, while the particles/film layer observed in the used sample were in the range 1-3 nm. A change in particle size towards a layer wetting the CNT surface during ECR explains the improved selectivity for HER over time, in accordance with the observations in Figure 2. Furthermore, the observed change in the value of α' from XPS (Figure S5) could be consistent with a reduction in particle size[29].

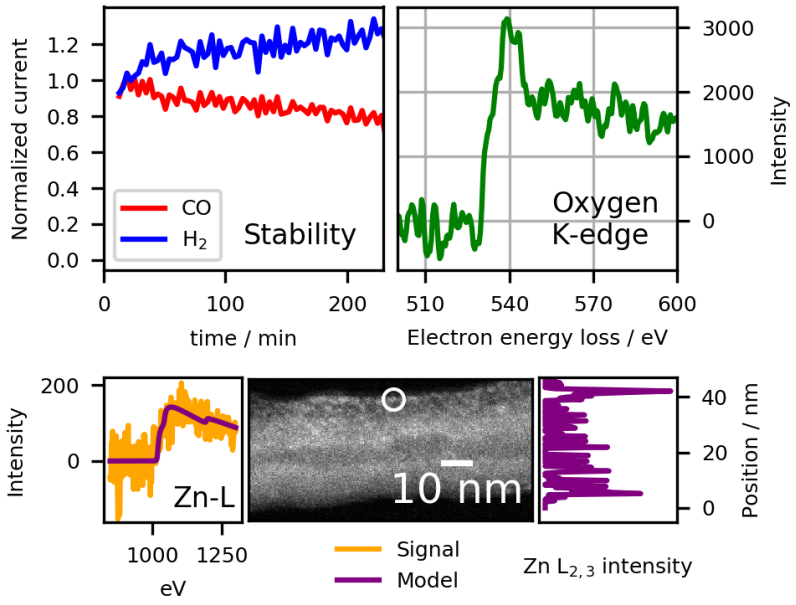

Figure 6. Stability of the synthesis gas composition, EEL spectra for oxygen and zinc acquired from a used catalyst and an ADF image of a used catalyst.

4. Conclusions

This work presents the carbon supported ZnO as a promising class of catalyst for active, cost effective and selective electrochemical reduction of CO_2 and H_2O to synthesis gas with a compositions suitable for Fischer-Tropsch synthesis. At moderate overpotentials, a Faradic efficiency of synthesis gas of more than 75% with a H_2/CO ratio close to 1 was achieved on small ZnO particles. The overpotential for the onset of synthesis gas was lower on smaller ZnO particle sizes. The H_2/CO ratio can be tailored by the ZnO particle size. The electrochemical CO_2 reduction activity is comparable to polycrystalline Ag, while DFT study revealed the ZnO surface is very active for CO_2 activation and stabilizes CO_2* and COOH* intermediates, which is more active than Ag (111) and Cu(111). While the catalytic activity of carbon supported ZnO catalyst is not as high as the recent oxide-derived Au and Ag, its cost is significantly lower and also selective for both electrochemical reduction of CO_2 and water. Therefore, this new class catalyst may provide a more practical platform for large-scale electrochemical reduction of CO_2 and H_2O simultaneously for sustainable synthesis gas generation. The cost is expected to be further reduced by choosing cheaper nanocarbon supports such as carbon black.

Keywords: electrochemical CO_2 reduction• ZnO •carbon nanofiber • syngas production